Preprints, 10th IFAC Symposium on Nonlinear Control Systems
August 23-25, 2016. Monterey, California, USA

Dynamic state-feedback control of nonlinear three-dimensional directional drilling systems

N. van de Wouw [*,**,***] **F.H.A. Monsieurs** [*] **E. Detournay** [**]

[*] *Department Mechanical Engineering, Eindhoven University of Technology, Eindhoven, Netherlands (e-mail: N.v.d.Wouw@tue.nl, f.h.a.monsieurs@hotmail.com)*
[**] *Department of Civil, Environmental & Geo- Engineering, University of Minnesota, Minneapolis, U.S.A. (e-mail: detou001@umn.edu)*
[***] *Delft Center for Systems and Control, Delft University of Technology, Delft, Netherlands*

Abstract: Directional drilling systems generate complex curved boreholes in the earth's crust for the exploration and harvesting of oil, gas and geothermal energy. In practice, boreholes drilled with such systems often show instability-induced borehole spiraling, which negatively affects the borehole quality and increases drag losses while drilling. This paper presents a dynamic state-feedback controller design approach for the stable generation of complex, three-dimensional borehole geometries, while avoiding undesired borehole spiraling. The design is based on a model for three-dimensional borehole propagation in terms of nonlinear delay differential equations. After casting the problem of borehole propagation into a tracking problem, it is shown that complex, three-dimensional borehole geometries can be asymptotically stabilized with the proposed controller. The effectiveness of the proposed approach is evidenced in an illustrative benchmark study.

Keywords: Directional drilling, tracking control, nonlinear systems, delay differential equations.

1. INTRODUCTION

The exploration and harvesting of hard-to-reach underground energy resources (such as oil, gas and geothermal energy) requires drilling complex curved boreholes. Directional drilling systems, including down-hole robotic systems known as rotary steerable systems (RSS), are used for this purpose. This work aims at the development of novel strategies for the control enabling three-dimensional borehole generation using such an RSS actuation mechanism.

Experimental evidence has shown that state-of-practice directional drilling (control) techniques can induce borehole oscillations, see e.g Marck et al. (2014). These oscillations in the borehole geometry are undesirable as they 1) compromise borehole stability, 2) reduce drilling efficiency), 3) reduce target accuracy, 4) make it more difficult to insert the borehole casing to prepare for production, and 5) reduce the rate-of-penetration (i.e. the speed of the drilling process). In this work, we aim to develop a model-based controller synthesis approach, which enables the drilling of complex three-dimensional (3D) borehole geometries while preventing borehole spiraling.

Several works exist on the topic of the control of directional drilling processes. In Panchal et al. (2012), controllers are developed based on empirical models of the borehole propagation process, in which a direct link between the force applied by the RSS and the curvature of the borehole is assumed. This approach ignores (physically relevant) transient behavior of the borehole propagation, which is essential in preventing borehole spiraling. In Bayliss and Matheus (2009), a state-space model for borehole propagation is derived and on the basis of this model, a controller is designed. However, the essential delay nature of the borehole propagation dynamics (see Neubert and Heisig (1996); Downton (2007); Perneder (2013)) is not captured in this model. In Sun et al. (2011), an $\mathcal{L}_1$ adaptive controller is designed, based on the directional drilling model of Downton (2007). In Kremers et al. (2015), a robust output-feedback approach for inclination control is proposed based on the model in Perneder (2013); Detournay and Perneder (2011).

All of the above control approaches focus on *two-dimensional* directional models, in which only the inclination dynamics is investigated. However, in practice complex *three-dimensional* borehole geometries need to be generated. Hence, control strategies applicable to three-dimensional directional drilling models are required that avoid undesired borehole spiraling effects. Compared to the two-dimensional case studied in the literature above, this is challenging due to the fact that existing three-dimensional models for directional drilling are described in terms of rather complex, multi-variable, nonlinear delay differential equations (DDEs).

The main contribution of this work is the development of a design strategy for controllers for three-dimensional direc-

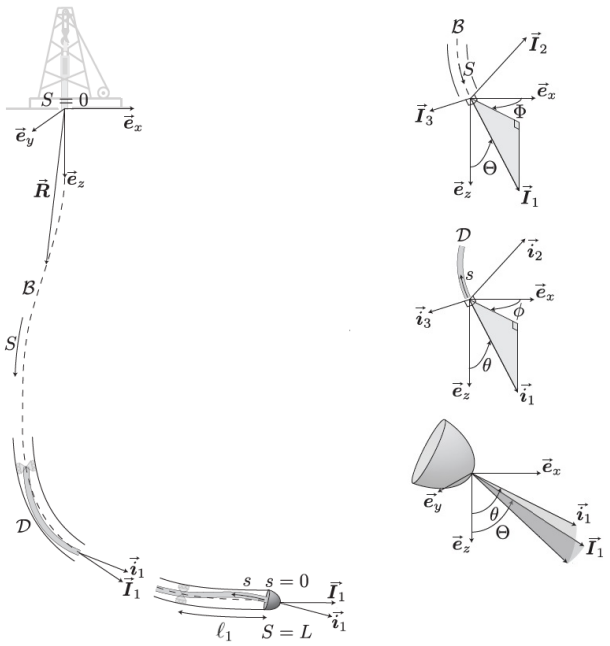

Fig. 1. Geometric description of the directional drilling system (left), borehole (top right), Bottom-Hole-Assembly (right middle) and bit (bottom right) (Perneder (2013)).

tional drilling systems. More detailed contributions are as follows. Firstly, the proposed method is based on a closed-form model description for three-dimensional borehole propagation, as proposed in Perneder (2013); Perneder and Detournay (2013b,a), which captures the essential, physically relevant, behavior of a three-dimensional directional drilling system. Secondly, unlike existing control methods, with Kremers et al. (2015) as an exception, the goal of the controller synthesis method is to design a controller which reduces borehole spiraling and prevents oscillations in the transient closed-loop response (both of which are detrimental to borehole quality). Thirdly, the proposed controller effectively deals with the nonlinear coupling between the inclination and azimuth dynamics characteristic to the dynamics of three-dimensional borehole propagation. Fourthly, a control strategy is proposed in which two identical and decoupled controllers for the inclination and azimuth dynamics are used, which simplifies the design and alleviates the burden of practical implementation.

2. 3D DIRECTIONAL DRILLING MODEL

As a basis for controller synthesis, we employ a three-dimensional, nonlinear model for directional drilling as developed in Perneder (2013); Perneder and Detournay (2013b,a). The schematic in Figure 1 (left figure) reflects that the directional borehole propagation process is primarily determined by the Bottom-Hole-Assembly (BHA), being the lowest part of the drill-string, which is laterally stabilized in the borehole by so-called stabilizers, and by the bit and rock properties. Figure 2 illustrates that the model comprises three main components. Firstly, the forces and moments acting on the bit are obtained by modeling the deformation of the BHA inside the borehole. Since the BHA is constrained in the borehole by the stabilizers in contact with the borehole wall, see Figure 1, the

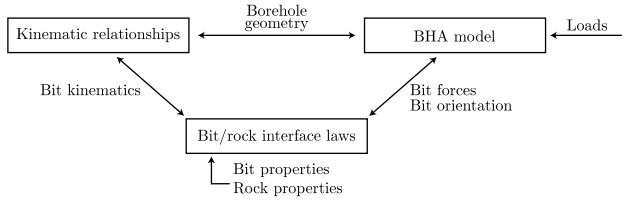

Fig. 2. Three components of the model and their interaction (Perneder and Detournay (2013b)).

existing borehole geometry affects the forces and moments on the bit in a spatially delayed manner. Secondly, the bit-rock interface law determines how these forces and moments on the bit are related to the penetration of the bit into the rock. Finally, the bit motion is related to the propagation of the borehole geometry through kinematic relationships.

2.1 Borehole evolution equations

This nonlinear model involves evolution equations for two angles fully describing the 3D borehole geometry: the borehole inclination Θ and the borehole azimuth Φ, as defined in Figure 1:

$$\eta\Pi\Big((\theta-\Theta)\cos\varpi+\sin\Theta\sin\varpi\,(\phi-\Phi)\Big)=\mathcal{F}_b\left(\theta-\langle\Theta\rangle_1\right)$$
$$+\mathcal{F}_w\Upsilon\sin\langle\Theta\rangle_1+\mathcal{F}_r\Gamma_\Theta+\sum_{i=1}^{n-1}\mathcal{F}_i\left(\langle\Theta\rangle_i-\langle\Theta\rangle_{i+1}\right),\quad(1a)$$
$$-\chi\Pi\theta'=\mathcal{M}_b\left(\theta-\langle\Theta\rangle_1\right)+\mathcal{M}_w\Upsilon\sin\langle\Theta\rangle_1+\mathcal{M}_r\Gamma_\Theta$$
$$+\sum_{i=1}^{n-1}\mathcal{M}_i\left(\langle\Theta\rangle_i-\langle\Theta\rangle_{i+1}\right),\quad(1b)$$
$$\eta\Pi\left(-\frac{(\theta-\Theta)\sin\varpi}{\sin\Theta}+\cos\varpi\,(\phi-\Phi)\right)=\mathcal{F}_b\left(\phi-\langle\Phi\rangle_1\right)$$
$$+\mathcal{F}_r\frac{\Gamma_\Phi}{\sin\Theta}+\sum_{i=1}^{n-1}\mathcal{F}_i\left(\langle\Phi\rangle_i-\langle\Phi\rangle_{i+1}\right),\quad(1c)$$
$$-\chi\Pi\phi'=\mathcal{M}_b\left(\phi-\langle\Phi\rangle_1\right)+\mathcal{M}_r\frac{\Gamma_\Phi}{\sin\Theta}$$
$$+\sum_{i=1}^{n-1}\mathcal{M}_i\left(\langle\Phi\rangle_i-\langle\Phi\rangle_{i+1}\right).\quad(1d)$$

In (1), $(\cdot)'$ indicates a derivative with respect to the (dimensionless) length of the borehole $\xi := L/l_1$ with L the length of the borehole and l_1 the distance between the bit and the first stabilizer, see Figure 1. Note that the independent variable in the model in (1) is the dimensionless spatial variable ξ. The variables θ and ϕ indicate the inclination and azimuth of the BHA, which differ from that of the borehole due to deformation of the BHA, see Figure 1. All angle variables in (1) are evaluated at the bit (in Figure 1 such variables are indicated with the $\hat{}$ symbol, which is omitted here for the sake of transparency). In (1), the average inclination and azimuth of the borehole in the i-th BHA segment (the segment between the $i-1$-th and i-th stabilizer, with $i=0$ indicating the bit) are given respectively as:

$$\langle\Theta\rangle_i := \frac{1}{\lambda_i}\int_{\xi_i}^{\xi_{i-1}}\Theta(\sigma)d\sigma,\ \langle\Phi\rangle_i := \frac{1}{\lambda_i}\int_{\xi_i}^{\xi_{i-1}}\Phi(\sigma)d\sigma,\quad(2)$$

which induces terms with distributed delays in (1). Herein, $\xi_i := \xi - \sum_{j=1}^{i} \lambda_j$ and $\lambda_j := l_j/l_1$ is the dimensionless length of the j-th BHA segment.

Let us now introduce the key model parameters. $\Pi = W_{act}/F_*$ denotes the dimensionless active weight-on-bit (which is assumed to be constant), with W_{act} the active weight on bit and $F_* := 3EI/l_1^2$ with EI denoting the BHA's bending stiffness. Moreover, ϖ is the so-called bit walk, the meaning of which is explained in Figure 3. Both the weight on bit Π and the bit walk angle ϖ are key parameters in the sense that these parameters strongly influence the dynamics (and determine whether borehole spiraling occurs) and in the sense that both parameters are subject to significant uncertainty in practice. The parameters η, χ are respectively the lateral and angular steering resistance of the bit. The number of stabilizers is given by n. The factors $\mathcal{F}$ and $\mathcal{M}$ in (1) (with appropriate indices) only depend on the specific configuration of the BHA, see Perneder (2013).

The term involving $\Upsilon \sin\langle\Theta\rangle_1$ in (1), with Υ a scaled measure of the BHA weight, is related to the influence of gravity on the BHA. We consider this term to be a (quasi-) constant perturbation, since the average inclination only changes slowly with the distance drilled. Finally, $\Gamma_i := \frac{F_{\mathrm{rss,i}}}{F_*}$, $i = \Theta, \Phi$, are the (scaled) RSS forces, i.e. the control inputs, where the RSS force vector $\vec{F}_{rss}$ is measured by the components $F_{rss,\Theta}$ and $F_{rss,\Phi}$ along the axes $\vec{I}_2$ and $\vec{I}_3$ respectively, see Figure 1.

The model in (1) consists of two nonlinear (delay) differential equations and two nonlinear (algebraic) constraint equations. To facilitate controller synthesis and given the fact that we are primarily interested in the borehole evolution (rather than in the BHA deformation), we eliminate the two constraint equations (and the BHA-related angles θ and ϕ) and arrive at a model in terms of two nonlinear delay differential equations in terms of the borehole-related variables Θ and Φ of the form:

$$\begin{aligned} \Theta'(\xi) &= f_\Theta(\Theta_\xi, \Phi_\xi, \Gamma_\Theta, \Gamma_\Phi, \Gamma_\Theta{}', \Gamma_\Phi{}'), \\ \Phi'(\xi) &= f_\Phi(\Theta_\xi, \Phi_\xi, \Gamma_\Theta, \Gamma_\Phi, \Gamma_\Theta{}', \Gamma_\Phi{}'), \end{aligned} \tag{3}$$

where $\Theta_\xi(\sigma) := \Theta(\xi + \sigma)$, $\Phi_\xi(\sigma) := \Phi(\xi + \sigma)$, for all $\sigma \in [\lambda_{tot}, 0]$ with $\lambda_{tot} = \sum_{i=1}^{n} \lambda_i$.

The expressions for f_Θ and f_Φ in (3) are rather complex and for details we refer to Monsieurs (2015).

2.2 Neutral bit walk model

The model significantly simplifies for the neutral bit walk case (i.e. $\varpi = 0°$). This parametric case will be employed for the purpose of the design of the structure of the

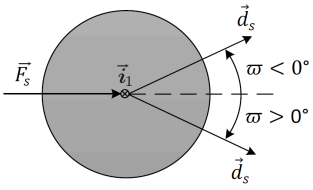

Fig. 3. The bit walk angle ϖ: the angle between the lateral force $\vec{F}_s$ and lateral penetration $\vec{d}_s$.

controller in Section 4 and in this case the model in (3) reads as

$$\begin{aligned} \chi\Pi\Theta' = &- \mathcal{M}_b(\Theta - \langle\Theta\rangle_1) + \frac{\chi}{\eta}\mathcal{F}_b(\Theta - \Theta_1) \\ &- \sum_{i=1}^{n-1} \frac{\mathcal{M}_b F_i + \mathcal{M}_i(\eta\Pi - \mathcal{F}_b)}{\eta\Pi}(\langle\Theta\rangle_i - \langle\Theta\rangle_{i+1}) \\ &- \frac{\chi}{\eta}\sum_{i=1}^{n-1}\mathcal{F}_i\left(\frac{\Theta_{i-1} - \Theta_i}{\lambda_i} - \frac{\Theta_i - \Theta_{i+1}}{\lambda_{i+1}}\right) \\ &- \frac{\mathcal{M}_b\mathcal{F}_r + (\eta\Pi - F_b)\mathcal{M}_r}{\eta\Pi}\Gamma_\Theta - \frac{\chi}{\eta}\mathcal{F}_r\Gamma_\Theta{}' + \mathcal{W}, \end{aligned} \tag{4}$$

with $\mathcal{W} := -\frac{\mathcal{M}_b\mathcal{F}_w + (\eta\Pi - \mathcal{F}_b)\mathcal{M}_w}{\eta\Pi}\Upsilon\sin\langle\Theta\rangle_1 - \frac{\chi}{\eta}\mathcal{F}_w(\Theta - \Theta_1)\Upsilon\cos\langle\Theta\rangle_1$ reflecting the effect of gravity, which is considered as a (quasi-) constant disturbance, and

$$\begin{aligned} \chi\Pi\Phi' = &- \mathcal{M}_b(\Phi - \langle\Phi\rangle_1) + \frac{\chi}{\eta}\mathcal{F}_b(\Phi - \Phi_1) \\ &- \sum_{i=1}^{n-1} \frac{\mathcal{M}_b F_i + \mathcal{M}_i(\eta\Pi - F_b)}{\eta\Pi}(\langle\Phi\rangle_i - \langle\Phi\rangle_{i+1}) \\ &- \frac{\chi}{\eta}\sum_{i=1}^{n-1}\mathcal{F}_i\left(\frac{\Phi_{i-1} - \Phi_i}{\lambda_i} - \frac{\Phi_i - \Phi_{i+1}}{\lambda_{i+1}}\right) \\ &+ \left(\frac{\chi}{\eta}\frac{\mathcal{F}_r\Theta'\cos\Theta}{(\sin\Theta)^2} - \frac{\mathcal{M}_b\mathcal{F}_r + \mathcal{M}_r(\eta\Pi - \mathcal{F}_b)}{\eta\Pi\sin\Theta}\right)\Gamma_\Phi \\ &- \frac{\chi}{\eta}\frac{\mathcal{F}_r}{\sin\Theta}\Gamma_\Phi{}'. \end{aligned} \tag{5}$$

Observe that the first three lines in the right-hand sides in (4) and (5) are identical and relate to the BHA being constrained in the borehole drilled in the past. The key differences between the inclination and azimuth dynamics, in (4) and (5), respectively, are twofold: 1) only the inclination dynamics is affected (nonlinearly) by gravity ($\mathcal{W}$ term) and 2) the inclination dynamics is decoupled from the azimuth dynamics; in contrast, the azimuth dynamics is influenced by the inclination dynamics in a nonlinear fashion through the terms involving the control input Γ_Φ and its spatial derivative.

3. CONTROL PROBLEM FORMULATION

The main goal of directional drilling is the generation of a borehole with some desired complex 3D geometry. In terms of the model in (4), (5) (or (3) in the non-neutral bit walk case), this objective can be formulated as a tracking problem. More specifically, we aim to track the inclination and azimuth reference trajectory $(\Theta_r(\xi), \Phi_r(\xi))$, for $\xi \in [-\lambda_{tot}, \infty]$. We assume that $\Theta_r(\xi)$ and $\Phi_r(\xi)$ are continuously differentiable, which is reasonable at the scale at which the problem is treated as it avoids curvature discontinuities. We aim to design a dynamic state-feedback controller such that the control inputs $\Gamma_i(\xi)$, $i = \Theta, \Phi$, render $(\Theta_r(\xi), \Phi_r(\xi))$ the asymptotically stable solution of the closed-loop system.

In addition, certain additional control objectives stem from the fact that the spiraling behavior in the borehole, which is often observed in practice, needs to be reduced/eliminated. Such borehole spiraling can either

be caused by poles in the right-half complex plane (i.e. instability), which is avoided if the state tracking problem is solved, or by undesired transient behavior. For this reason, we also focus on achieving improved transient behaviour in order to reduce/eliminate transient borehole spiraling. Another control objective is related to the fact that robustness to slowly changing gravity-induced forces is required.

4. CONTROLLER DESIGN

The structural design of the controller introduced next is based on the neutral bit walk model in (4) and (5). Later, also the performance of this controller will be considered for both the neutral and non-neutral bit walk cases. Without loss of generality, we focus on a two-stabiliser case here (i.e. $n = 2$).

4.1 Controller structure

The structure of the proposed controller strategy is schematically depicted in Figure 4, which consists of the following components: 1) Decoupling input transformation, 2) Input filters, 3) Combined feedforward and dynamic state-feedback tracking controller, which are subsequently discussed in more detail.

Decoupling input transformation The borehole propagation dynamics in (4) and (5) (i.e. for neutral (zero) bit walk) is coupled (from inclination to azimuth dynamics) in a nonlinear fashion through the input (i.e. RSS force) related terms. We introduce new control inputs Γ^*_Θ and Γ^*_Φ, defined through the following input transformation:

$$\begin{bmatrix}\Gamma_\Theta\\ \Gamma_\Phi\end{bmatrix} = \begin{bmatrix}1 & 0\\ 0 & \sin\Theta\end{bmatrix}\begin{bmatrix}\Gamma^*_\Theta\\ \Gamma^*_\Phi\end{bmatrix}, \tag{6}$$

for $\Theta \in (0, \pi)$, such that

$$\begin{bmatrix}\Gamma'_\Theta\\ \Gamma'_\Phi\end{bmatrix} = \begin{bmatrix}\Gamma^{*\prime}_\Theta\\ \Gamma^{*\prime}_\Phi \sin\Theta + \Gamma^*_\Phi \Theta' \cos\Theta\end{bmatrix}, \tag{7}$$

This input transformation achieves decoupling of the inclination and azimuth dynamics, which, after the input transformation, satisfy the following first-order linear DDEs:

$$\begin{aligned} z'_i(\xi) =& A_{z0} z_i(\xi) + A_{z1} z_i(\xi_1) + A_{z2} z_i(\xi_2) \\ &+ B_{z0}\Gamma^*_i + B_{z1}\Gamma^{*\prime}_i + \mathcal{W}_i, \end{aligned} \tag{8}$$

for $i = \{\Theta,\ \Phi\}$, where $\mathcal{W}_\Theta = \mathcal{W}$, $\mathcal{W}_\Phi = 0$, and where the system matrices (A_{z0}, A_{z1} and A_{z2}) and the input matrices (B_{z0} and B_{z1}) are defined by (9). In fact, the inclination and azimuth dynamics are now not only decoupled but also identical (apart from the gravity related disturbance term $\mathcal{W}$), which simplifies the controller design (and practical implementation) in the sense that inclination and azimuth controllers for Γ_Θ and Γ_Φ can be the same. In (8), the state vectors z_i, $i \in \{\Theta, \Phi\}$, are given by $z_\Theta = [\Theta,\ \langle\Theta\rangle_1,\ \langle\Theta\rangle_2]^T$ and $z_\Phi = [\Phi,\ \langle\Phi\rangle_1,\ \langle\Phi\rangle_2]^T$. Extending the state with the average inclinations and azimuths supports the description of the dynamics with DDE involving point-wise delays (as opposed to distributed delays).

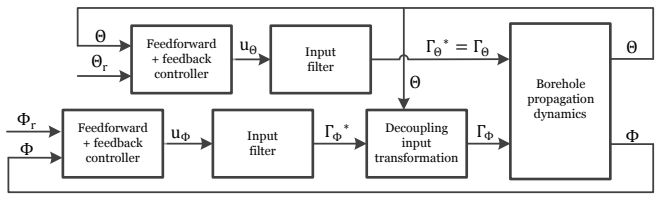

Fig. 4. Schematic overview of the control structure.

Input filters In support of the tracking controller design, discussed in the next section, input filters, see Figure 4, are included in the design:

$$\Gamma^{*\prime}_i = -\frac{b_{z0}}{b_{z1}}\Gamma^*_i + \frac{1}{b_{z1}}u_i, \tag{10}$$

where b_{z0} and b_{z1} are the first entries of the vectors B_{z0} and B_{z1} (i.e. $B_{z0} = [b_{z0},\ 0,\ 0]^T$ and $B_{z1} = [b_{z1},\ 0,\ 0]^T$). Applying these input filters to (8) yields

$$z'_i(\xi) = A_{z0} z_i(\xi) + A_{z1} z_i(\xi_1) + A_{z2} z_i(\xi_2) + B_z u_i + \mathcal{W}_i, \tag{11}$$

for $i = \{\Theta,\ \Phi\}$ and with $B_z = [1\ 0\ 0]^T$.

Tracking controller The tracking controller proposed here consists of a feedforward part $u_{r,i}$ and feedback part $u_{fb,i}$, i.e. $u_i = u_{r,i} + u_{fb,i}$, where the feedforward controller is given by

$$u_{r,i} = B_z^+\left(z'_{r,i}(\xi) - A_{z0} z_{r,i}(\xi) - A_{z1} z_{r,i}(\xi_1) - A_{z2} z_{r,i}(\xi_2)\right), \tag{12}$$

where B_z^+ $(= [1,\ 0,\ 0])$ denotes the pseudoinverse of the vector B_z, $z_{r,\Theta}(\xi) = [\Theta_r(\xi),\ \langle\Theta_r\rangle_1(\xi),\ \langle\Theta_r\rangle_2(\xi)]^T$ and $z_{r,\Phi}(\xi)$ defined similarly [1]. The dynamic state-feedback tracking controller is designed as follows:

$$\begin{aligned} p'_i &= A_{c,i} p_i + B_{c,i}(z_i - z_{r,i}), \\ u_{fb,i} &= C_{c,i} p_i, \end{aligned} \tag{13}$$

where

$$A_{c,i} = \begin{bmatrix}0 & 0\\ \gamma_i & -\gamma_i\end{bmatrix},\ B_{c,i} = \begin{bmatrix}\zeta_i[k_{1,i},\ 0,\ 0]\\ \gamma_i K_{p,i}\end{bmatrix},\ C_{c,i} = [0,\ 1], \tag{14}$$

for $i = \{\Theta,\ \Phi\}$. The proportional feedback gain matrices are defined by $K_{p,i} := [k_{1,i},\ k_{2,i},\ k_{3,i}]$ for $i = \{\Theta,\ \Phi\}$. Integral action is added to the controller to eliminate the effects of (quasi-)constant (gravity-induced) disturbances (i.e. to remove steady-state errors), where the parameter ζ_i determines the cut-off frequency of the integral action. In order to reduce/avoid oscillations on the short range length scale ($\xi = \mathcal{O}(10^{-1})$), the controller contains also a low-pass filter. The dynamics on the short-range can be excited when the reference trajectory quickly changes (for instance a transition from straight to curved borehole section) or when the controller instantly reacts to an (initial) error between the states and reference, thereby inducing undesired borehole kinking. A second reason to include a low-pass filter in the controller is to be less sensitive for measurement noise in practice. The cut-off frequency of this low-pass filter is determined by the parameter γ_i.

4.2 Controller tuning

To support controller gain tuning, the following closed-loop error dynamics is obtained, with $e_i = z_i - z_{r,i}$:

$$\begin{aligned} \begin{bmatrix}e'_i(\xi)\\ p'_i(\xi)\end{bmatrix} &= \begin{bmatrix}A_{z0} & B_z C_{c,i}\\ B_{c,i} & A_{c,i}\end{bmatrix}\begin{bmatrix}e_i(\xi)\\ p_i(\xi)\end{bmatrix} + \begin{bmatrix}A_{z1} & 0\\ 0 & 0\end{bmatrix}\begin{bmatrix}e_i(\xi_1)\\ p_i(\xi_1)\end{bmatrix} \\ &+ \begin{bmatrix}A_{z2} & 0\\ 0 & 0\end{bmatrix}\begin{bmatrix}e_i(\xi_2)\\ p_i(\xi_2)\end{bmatrix}. \end{aligned} \tag{15}$$

[1] The gravity effect is not accounted for in the feedforward design; integral action in the feedback design effectively deals with the (quasi-) constant gravity-related disturbance.

$$A_{z0} = \frac{1}{\chi\Pi}\begin{bmatrix} -\mathcal{M}_b + \frac{\chi}{\eta}(\mathcal{F}_b - \mathcal{F}_1) & \mathcal{M}_b - \mathcal{M}_1 + \frac{\mathcal{F}_b\mathcal{M}_1 - \mathcal{F}_1\mathcal{M}_b}{\eta\Pi} & \mathcal{M}_1 + \frac{(-\mathcal{F}_b\mathcal{M}_1 + \mathcal{F}_1\mathcal{M}_b)}{\eta\Pi} \\ \chi\Pi & 0 & 0 \\ 0 & 0 & 0 \end{bmatrix},$$

$$A_{z1} = \frac{1}{\chi\Pi}\begin{bmatrix} \frac{\chi}{\eta}(\mathcal{F}_1 + \frac{\mathcal{F}_1}{\lambda_2} - \mathcal{F}_b) & 0 & 0 \\ -\chi\Pi & 0 & 0 \\ \frac{\chi\Pi}{\lambda_2} & 0 & 0 \end{bmatrix}, \quad A_{z2} = \frac{1}{\chi\Pi}\begin{bmatrix} -\frac{\chi\mathcal{F}_1}{\eta\lambda_2} & 0 & 0 \\ 0 & 0 & 0 \\ -\frac{\chi\Pi}{\lambda_2} & 0 & 0 \end{bmatrix}, \tag{9}$$

$$B_{z0} = \frac{1}{\chi\Pi}\left[-\mathcal{M}_r + \frac{1}{\eta\Pi}(\mathcal{F}_b\mathcal{M}_r - \mathcal{F}r\mathcal{M}_b),\ 0,\ 0\right]^T, \quad B_{z1} = \frac{1}{\chi\Pi}\left[-\frac{\chi}{\eta}\mathcal{F}_r,\ 0,\ 0\right]^T.$$

These error dynamics is globally asymptotically stable (thereby achieving the tracking control objective) if and only if the right-most closed-loop pole is located in the left-half complex plane. The convergence rate of the transient response towards the desired borehole trajectory will be largely determined by the (maximum) real part of the closed-loop poles. Therefore, the controller gains are designed by solving the following minimization problem

$$\min_{K_{p,i},\, i\in\{\Theta,\Phi\}} \alpha(K_{p,\Theta}, K_{p,\Phi}), \tag{16}$$

with

$$\alpha(K_{p,\Theta}, K_{p,\Phi}) = \max_{j\in[1,2,\ldots,\infty]} \{\Re(s_j(K_{p,\Theta}, K_{p,\Phi}))\}, \tag{17}$$

and $s_j(K_{p,\Theta}, K_{p,\Phi})$ the (infinitely many) closed-loop poles of the tracking error dynamics (15) induced by the controller gains $K_{p,\Theta}$, $K_{p,\Phi}$. Herewith, we pursue a pole placement technique (for DDEs) towards stabilization, see Michiels and Niculescu (2007). Note that because the tracking error dynamics associated with the inclination and azimuth dynamics are identical and decoupled, we can choose $K_{p,\Theta} = K_{p,\Phi} =: K_p$, which simplifies the above optimization problem. The problem of finding the gain matrix K_p is a non-smooth optimization problem. This problem can be solved using a gradient sample algorithm, see Burke et al. (2005). Prior to performing this optimization process, the parameters for the low-pass filter and integral action (γ_i and ζ_i) are fixed. These parameters are not designed together with the gain matrix $K_{p,i}$ through the above optimization-based approach, because the input filter and the integral action pursue control objectives on other length scales than the feedback controller (the short and long length scales, respectively); the tracking goal objective should be achieved on the medium-range length scale.

5. ILLUSTRATIVE BENCHMARK STUDY

5.1 Benchmark problem definition

The BHA in this benchmark system is equipped with two stabilizers ($n = 2$), illustrated in Figure 5. Table 1 specifies the complete BHA geometry of the benchmark system. The BHA consists of pipes with an inner and outer radius I_r and O_r given in this table, and the area moment of inertia of the BHA is $I = \pi/4 \cdot (O_r^4 - I_r^4) = 3.6 \cdot 10^{-5}$ m^4. The BHA's is made of steel with a Young's modulus $E_y = 2 \cdot 10^{11}$ N/m^2; hence, the characteristic force F_* in this benchmark system is equal to $1.6 \cdot 10^6$ N. The dimensionless parameters of the BHA configuration (λ_1, λ_2, Λ) corresponding to benchmark system described above are given in Table 2, where Λ characterizes the location of the RSS, see Figure 5. The dimensionless lateral and angular steering resistance η and χ of the benchmark system, see Table 2, are chosen corresponding to a bit with a rather long passive gauge. Given the material density of the BHA pipes ($\rho = 7800$ kg/m^3 for steel), the distributed weight w of the BHA is $w = 1.08 \cdot 10^3$ N/m, which corresponds to a dimensionless distributed weight Υ as given in Table 2. We consider a desired 3D borehole geometry consisting of three sections: a vertical section without curvature (so a straight line), followed by a curved section and a straight horizontal section, see Figure 6.

5.2 A neutral bit walk case study

Let us first consider the nominal case for $\varpi = 0°$ (i.e. zero (neutral) bit walk) and $\Pi = 0.0087$. Using the controller design and tuning strategy described in Section 4, we arrive at the following controller gains: $K_p = [2654\ 1256;\ 289]$, and $\zeta_i = 0.5$, $\gamma_i = 0.8$, for $i \in \{\Theta, \Phi\}$. In doing so, the optimization-based tuning strategy was terminated when $\alpha(K_p, K_p) \leq 0.5$. In Figure 7, the closed-loop poles (and the open-loop poles) are displayed, which shows that this controller indeed stabilizes the desired trajectory. Note that the open-loop system has a real pole in zero. The latter fact is further evidenced by the simulation results involving the tracking errors in Figure 8, for initial borehole inclination and azimuth given by $\Theta_\xi(0) = 2.5°$ and $\Phi_\xi(0) = 100.5°$. The simulations are carried out with the nonlinear directional drilling model in (4), (5) including the influence of gravity. This figure shows that the closed-loop tracking errors asymptotically converge to zero within a length scale of $\xi = 10$ and that the tracking control objective is achieved without undesirable transient effects such as borehole spiraling and kinks. The integral action of the controller indeed ensures zero steady-state error (although the gravity-induced force disturbance is present). This figure also depicts an open-loop response for which the feedforward (and the decoupling law) are still employed. In contrast to the closed-loop response, the open-loop inclination error response shows a drift caused by gravity-induced disturbance (which does not affect the azimuth dynamics). In the absence of gravity-related disturbances, both the open-loop inclination and azimuth error would remain constant (and typically non-zero) due to the presence of the pole at zero in the open-loop dy-

Table 1. The BHA geometry of the benchmark system.

ℓ_1	ℓ_2	$\Lambda\ell_1$	I_r	O_r
3.66 m	6.10 m	0.61 m	0.0533 m	0.0857 m

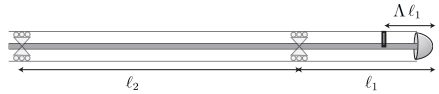

Fig. 5. The BHA configuration of the benchmark system.

Table 2. Parameters of the benchmark system.

λ_1	λ_2	Λ	χ	η	Υ
1	1.667	0.167	0.1	30	0.0024

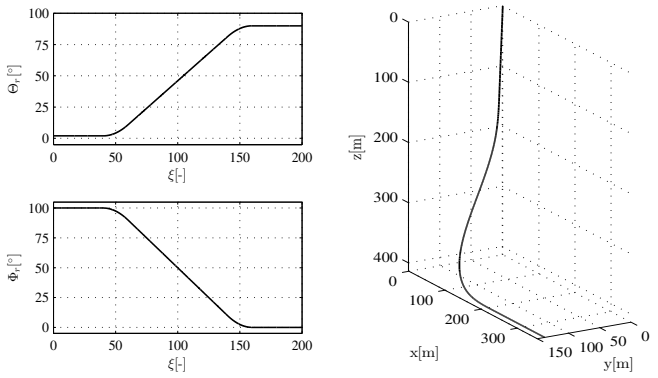

Fig. 6. The reference trajectory expressed in the borehole inclination and azimuth (figures on the left), and visualized in Cartesian coordinates (right figure).

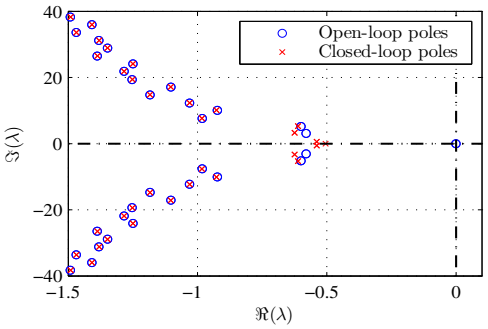

Fig. 7. Open and closed-loop poles for $\Pi = 0.0087$ and $\varpi = 0°$ controlled by the neutral bit walk control strategy.

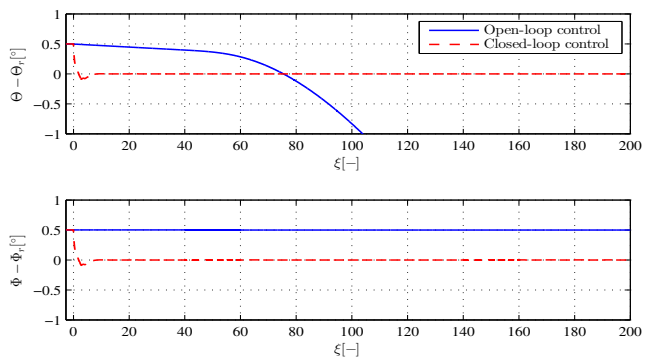

Fig. 8. Error response using the neutral bit walk control strategy and for the open-loop system including decoupling law, input filter and feedforward, for $\varpi = 0°$ and $\Pi = 0.0087$.

namics (in combination with the perfect feedforward still employed in the open-loop simulation)

6. CONCLUSIONS

This paper has proposed a dynamic state feedback control strategy for three-dimensional borehole propagation in directional drilling. The problem of generating a desired three-dimensional borehole geometry is recast into a tracking problem in terms of inclination and azimuth (angle) variables describing the (desired) borehole geometry. Based on a model in terms of nonlinear delay differential equations, as developed in Perneder (2013), we have proposed to design the controller solving this tracking problem based on a neutral bit walk model, which allows to fully decouple the inclination and azimuth dynamics. The latter approach simplifies the tracking controller design and tuning and alleviates the burden of implementation of such controllers. An illustrative benchmark study has evidenced the effectiveness of the proposed approach.

REFERENCES

Bayliss, M. and Matheus, J. (2009). Directional drilling tool simulation and system design. *SAE Int. J. Mater. Manuf.* doi:10.4271/2008-01-1369.

Burke, J., Lewis, A., and Overton, M. (2005). *A robust gradient sampling algorithm for nonsmooth,nonconvex optimization.* SIAM J. Optim. ISSN: 10526234.

Detournay, E. and Perneder, L. (2011). Dynamical model of a propagating borehole. *Proceedings of the 7th ENOC Conference, Rome, Italy.*

Downton, G. (2007). Directional drilling system response and stability. In *Proceedings of the IEEE Int. Conference on Control Applications*, 1543 –1550.

Kremers, N., Detournay, E., and van de Wouw, N. (2015). Model-based robust control of directional drilling systems. *IEEE Transactions on Control Systems Technology*, 24(1), 226–239.

Marck, J., Detournay, E., Kuesters, A., and Wingate, J. (2014). Analysis of spiraled borehole data using a novel directional drilling model. *SPE Drilling and Completion*, (SPE167992), 267–278.

Michiels, W. and Niculescu, S. (2007). *Stability and Stabilization of Time-Delay Systems, An Eigenvalue-Based Approach.* SIAM.

Monsieurs, F. (2015). *Model-based decoupled control of a 3D directional drilling system.* Master's thesis, DC 2015.064, Eindhoven University of Technology, the Netherlands.

Neubert, M. and Heisig, G. (1996). Mathematical description of the directional drilling process and simulation of directional control algorithm. *ZAMM*, 76, 361–362.

Panchal, N., Bayliss, M., and Whidborne, J. (2012). Attitude control system for directional drilling bottom hole assemblies. *IET Control Theory and Applications*, 6, 884–892.

Perneder, L. and Detournay, E. (2013a). Equilibrium inclinations of straight boreholes. *SPE Journal*, 18(3), 395–405.

Perneder, L. and Detournay, E. (2013b). Steady-state solutions of a propagating borehole. *International Journal of Solids and Structures*, 50, 1226–1240.

Perneder, L. (2013). *A Three-Dimensional Mathematical Model of Directional Drilling.* Ph.D. thesis, University of Minnesota, Minneapolis, U.S.A.

Sun, H., Li, Z., Hovakimyan, N., Basar, T., and Downton, G. (2011). L1 adaptive control for directional drilling systems. *Automatic Control in Offshore Oil and Gas Production*, 1, 72–77.